

The combined effects of North Atlantic Oscillation and Western Pacific teleconnection on winter temperature in Eastern Asia during 1980–2021

Ziqun Zhang^{1,3}, Hongyan Cui^{1,3*}, Baoxu Chen^{1,3}, Hong Cai^{1,3}, Pin Li²

¹ College of Mathematics and Physics, Qingdao University of Science and Technology, Qingdao 266061, China

² The First Institute of Oceanography, Ministry of Natural Resources, Qingdao 266061, China

³ Research Institute for Mathematics and Interdisciplinary Sciences, Qingdao University of Science and Technology, Qingdao 266061, China

Received 3 February 2023; accepted 6 April 2023

© Chinese Society for Oceanography and Springer-Verlag GmbH Germany, part of Springer Nature 2023

Abstract

As important atmospheric circulation patterns in Northern Hemisphere (NH), the North Atlantic Oscillation (NAO) and the Western Pacific teleconnection (WP) affect the winter climate in Eurasia. In order to explore the combined effects of NAO and WP on East Asian (EA) temperature, the NAO and WP indices are divided into four phases from 1980–2021: the positive NAO and WP phase (NAO+/WP+), the negative NAO and WP phase (NAO-/WP-), the positive NAO and negative WP phase (NAO+/WP-), the negative NAO and positive WP phase (NAO-/WP+). In the phase of NAO+/WP+, the low geopotential height (GH) stays in north of EA at 50°–80°N; the surface air temperature anomaly (SATA) is 0.8–1 °C lower than Southern Asian. In the phase of NAO-/WP-, the center of high temperature and GH locate in the northeast of EA; the cold air spreads to Southern Asia, causing the SATA decreases 1–1.5 °C. In the phase of NAO+/WP-, the high GH belt is formed at 55°–80°N. Meanwhile, the center of high SATA locates in the north of Asia that increases 0.8–1.1 °C. The cold airflow causes temperature dropping 0.5–1 °C in the south of EA. The SATA improves 0.5–1.5 °C in south of EA in the phase of NAO-/WP+. The belt of high GH is formed at 25°–50°N, and blocks the cold air which from Siberia. The NAO and WP generate two warped plate pressure structures in NH, and affect the temperature by different pressure configurations. NAO and WP form different GH, and GH acts to block and push airflow by affecting the air pressure, then causes the temperature to be different from the north and south of EA. Finally, the multiple linear regression result shows that NAO and WP are weakened by each other such as the phase of NAO+/WP+ and NAO-/WP-.

Key words: North Atlantic Oscillation (NAO), Western Pacific teleconnection (WP), winter temperature, combined effect, Eastern Asia

Citation: Zhang Ziqun, Cui Hongyan, Chen Baoxu, Cai Hong, Li Pin. 2023. The combined effects of North Atlantic Oscillation and Western Pacific teleconnection on winter temperature in Eastern Asia during 1980–2021. *Acta Oceanologica Sinica*, 42(10): 1–9, doi: 10.1007/s13131-023-2187-6

1 Introduction

The North Atlantic Oscillation (NAO) and the Western Pacific teleconnection (WP) are located in the North Atlantic Ocean and the West Pacific Ocean (Wibig, 1999). NAO appears as typical north-south dipole modes and it relates to the pressure and temperature (Hurrell, 1995). In positive phase of NAO, Northern and Central Europe are warm and the Mediterranean is cold. During the negative phase of NAO, a weak subtropical high and a weak Icelandic low cause moist air gets into the Mediterranean and cold air gets into northern Europe (Hurrell et al., 2003; Rousi et al., 2020). Abnormal NAO can bring blizzard and extreme cold, causing heavy rain and freezing disasters (Hori, 2003; Yao and Luo, 2016). At the same time, the Eastern Asia Surface Air Temperature (SAT) is closely associated with the NAO (Li and Wang,

2003; Li et al., 2022). Abnormal NAO can cause temperature to decrease in Southeastern China (Wang and Shi, 2001).

Wallace and Gutzler (1981) identified the WP pattern is one of the most important components of atmospheric circulation correlated with SAT teleconnections over Eastern Asia. Positive phase of WP affects temperature warm in south of Asia. The negative phase of WP affects the Eastern Asia monsoon and leads to temperature decrease over Eastern Asia in the winter (Gong et al., 2001; Zhang et al., 2009). The pattern of WP can be related to ENSO during the winter (Bell et al., 2009; Chen et al., 2013; Oshika et al., 2015). As an important phenomenon to impact on the global climate, ENSO has a complex association with WP (Shi and Zhu, 1993). Some scholars tried to study some low-frequency, extratropical teleconnection patterns, such as NAO, to

Foundation item: The National Key Research and Development Program of China under contract No. 2022YFE0140500; the National Natural Science Foundation of China under contract Nos 41821004 and 42130406; the National Natural Science Foundation of China-Shandong Joint Fund under contract No. U1906215; the Open Fund of Key Laboratory of Ocean Circulation and Waves, Chinese Academy of Sciences under contract No. KLOCW2003; the Project of Doctoral Found of Qingdao University of Science and Technology under contract No. 210010022746.

*Corresponding author, E-mail: cuihy@qust.edu.cn

build a composite statistical model to predict SAT (Feldstein, 2000; Saunders and Qian, 2002; Dai et al., 2017; Yoo et al., 2018). In recent years, studies on the combination of NAO-WP phases begin to appear. It is reported that it has a complex relationship between NAO, ENSO and WP through statistical analyses (Oshika et al., 2015; Nakamura et al., 2015). Park and Ahn (2016) explore the combined effect of the Arctic Oscillation (AO) and the WP on winter temperature, they proposed an index considering the effect of both AO and WP on East Asia winter temperature. The correlation between the index and the East Asia winter temperature was statistically significant at the 99% confidence level. This provides a good demonstration for exploring the relationship between NAO and WP. Shi et al. (2021) indicate that different NAO-WP phases have different effects on winter temperatures in southern China. But the combination of NAO and WP at low index levels is not discussed. In addition, the structure about the combined effects of the NAO and WP has not been clearly summarized. We hope to further discuss the combined effects of the air pressure warping structures on Eurasian continent. Meanwhile, we straighten out the relationships among geopotential height (GH), wind and SAT under the NAO-WP. The mechanisms of the combined action of NAO-WP are deeply discussed.

In this paper, the NAO and WP are divided into four phases of 1980–2021, in order to study the distribution of temperature in winter. Calculating the SAT anomaly (SATA) to explain the characteristics in the four phases of NAO-WP. We introduce the data and methods in Section 2 and present the results in Section 3. Conclusions and discussion are in Section 4.

2 Data and methods

2.1 Data

The monthly indices of NAO and WP are from National Oceanic and Atmospheric Administration (NOAA) Climate Prediction Center, obtained from the website of the Climate Indices List.

We use the air temperature data from NOAA-20th Century Reanalysis database version 3, on a global $2.5^\circ \times 2.5^\circ$ latitude-longitude grid from December 1979 to February 2021. The atmospheric data of GH, Horizontal Wind Component and Vertical Wind Component are obtained from National Centers for Environmental Prediction (NCEP) Reanalysis Database (Reanalysis-2), which the spatial resolutions of $2.5^\circ \times 2.5^\circ$, and the temporal coverage is from December 1979 to February 2021.

In this paper, the season of Northern Hemisphere (NH) is divided by this: the spring includes March, April and May (MAM), the summer includes June, July and August (JJA), the autumn includes September, October and November (SON), while the winter includes December, January and February (DJF).

2.2 Identification of four phases to NAO-WP

This study averages the NAO and WP indices as a value in each winter of 1980–2021. The time series of NAO and WP indices are shown in Fig. 1a.

The positive values of NAO are 32 years and the positive WP indices are 22 years from 1980 to 2021 (Fig. 1a). The negative values of NAO have 10 years and the negative WP indices have 20 years from 1980 to 2021 (Fig. 1a). According to the positive and

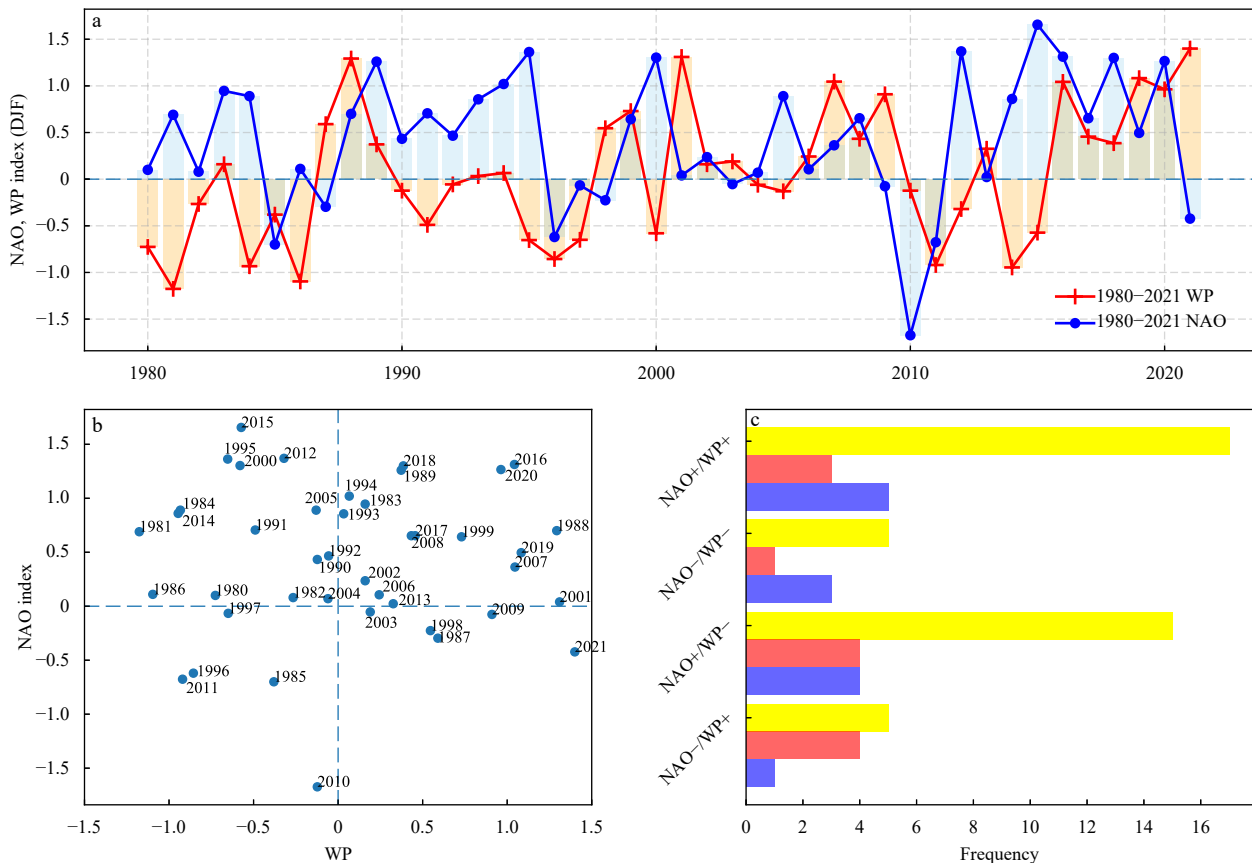


Fig. 1. The NAO and WP indices in winter 1980–2021 (a); the four phases of NAO-WP (b); the frequency of NAO-WP (c). The yellow bar represents the total frequency of the different phases; the red bar represents the frequency of El Niño year; and the blue bar represents the frequency of La Niña year.

negative characteristics of NAO and WP, the indices are divided into four phases (Fig. 1b). The positive value of NAO and WP phase (NAO+/WP+) at the same time have 17 years including 1983, 1988, 1989, 1993, 1994, 1999, 2001, 2002, 2006, 2007, 2008, 2013, 2016, 2017, 2018, 2019 and 2020 (Table 1). Among them, El Niño year accounted for 17.6%, La Niña year accounted for 29.4% (Figs 1b and c); the negative NAO and WP phase (NAO-/WP-) have 5 years including 1985, 1996, 1997, 2010 and 2011, El Niño year accounted for 20%, La Niña year accounted for 60% (Figs 1b and c); the positive NAO and negative WP phase (NAO+/WP-) have 15 years including 1980, 1981, 1982, 1984, 1986, 1990, 1991, 1992, 1995, 2000, 2004, 2005, 2012, 2014 and 2015. Among them, El Niño year accounted for 26.6%, La Niña year accounted for 26.6% (Figs 1b and c); the negative NAO and positive WP phase (NAO-/WP+) have 5 years including 1987, 1998, 2003, 2009 and 2021, El Niño year accounted for 80%, La Niña year accounted for 20% (Figs 1b and 1c). From the frequency of occurrence, the phase of NAO+/WP+ occurred most frequently, which has 17 times. The phase of NAO+/WP- occurred 15 times. NAO-/WP- and NAO-/WP+ occurred less frequently, only five times, respectively.

2.3 Method of Multiple linear regression

Multiple regression analysis is often used to analyze the relationship for variables. This study analyzes the relationship between SAT and NAO-WP indices by multiple regression. The time series T_i are the SAT which in the four phases of NAO-WP, the sample length is the number of years selected for each phase, and the regression equation is

$$T_i = aI_{NAO} + bI_{WP} + \varepsilon, \quad (1)$$

where gradient a and b represent the change of temperature, I_{NAO} represents the NAO index, I_{WP} represents the WP index, the ε is error. The coefficients of a and b are calculated as follows:

$$a = \frac{\sum_{i=1}^n T_i I_{NAO} - \frac{1}{n} \left(\sum_{i=1}^n T_i \right) \left(\sum_{i=1}^n I_{NAO} \right)}{\sum_{i=1}^n I_{NAO}^2 - \frac{1}{n} \left(\sum_{i=1}^n I_{NAO} \right)^2}, \quad (2)$$

$$b = \frac{\sum_{i=1}^n T_i I_{WP} - \frac{1}{n} \left(\sum_{i=1}^n T_i \right) \left(\sum_{i=1}^n I_{WP} \right)}{\sum_{i=1}^n I_{WP}^2 - \frac{1}{n} \left(\sum_{i=1}^n I_{WP} \right)^2}, \quad (3)$$

$$\varepsilon = \frac{1}{n} \sum_{i=1}^n T_i - \frac{a}{n} \sum_{i=1}^n I_{NAO} - \frac{b}{n} \sum_{i=1}^n I_{WP}. \quad (4)$$

2.4 Method of empirical orthogonal function analysis

Monthly 500 hPa air temperature variations during DJF for

the period of 1980–2021 are adopted in this study to examine atmospheric circulation patterns associated with the phase of NAO-WP in Eastern Asia. Empirical orthogonal function analysis (EOF) is used to analyze the spatial and temporal variability of single geophysical fields (Thompson and Wallace, 1998). The space–time decomposition is $X = EOF_{n \times n} \times PC_{n \times m}$, which n refers to the location in space, m indicates the length of the time series, EOF corresponds to the spatial patterns of variability, and PC is the principal component (PC) and corresponds to the temporal patterns of variability. Here, we separate the spatial distribution mode of the original temperature field from the time series. The spatial distribution mode is only a function of the space, and the time series is given in the form of PC value. First, we calculate the monthly 500 hPa air temperature anomalies and relative to the climatological mean values for 1980–2021. Second, air temperature anomalies are weighted by latitude. Then, we calculate the monthly 500 hPa air temperature anomalies during DJF for the period of 1980–2021. A span of 126 months are used to perform the EOF analysis, then extract spatial modes and the correspond time series.

3 Results

3.1 The surface air temperatures anomaly in four phases

In order to explain the characteristics of the four phases about NAO-WP, we calculate the SATA from 1980 to 2021 in the NH (Fig. 2).

In the phase of NAO+/WP+, the SATA is lower in the north of Eastern Asian area (50°–70°N, 100°–170°E) than the south of Asian (20°–40°N, 90°–130°E) (Fig. 2a). A cold center forms over Kamchatka with the SATA decreasing about 0.5–0.8°C. The negative WP corresponds to low temperature and weak pressure field in this area. The SATA is increased in the other area of Eurasia. In the North Atlantic, the distribution of SATA is similar to the Kamchatka. In these areas, NAO and WP seem to play the same role. In the phase of NAO-/WP- (Fig. 2b), the distribution of SATA is the opposite to the NAO+/WP+ phase. A low SATA zone which through Eurasia is formed around 30°–80°N. That means the winter is cold in south of Eastern Asia. The Northern Europe and Siberia decrease 2–3°C, and the Eastern Kamchatka increases 1–2°C (Fig. 2b). The negative NAO weakens the jet stream on the Atlantic, it makes the mid-latitudes of Europe cold and dry. The role of WP in Eastern Asia is also reflected in the cooling of the southern region.

The SATA decreases 0.5–0.8°C at the south of Eastern Asia in the phase of NAO+/WP- (Fig. 2c). The SATA improves 0.5–0.8°C in the north of Eastern Asia, which forms a warm center. Another warm center is formed in the Ural region with SATA improving 0.8–1.1°C. The temperature is high in northern Asia, while it is low in the south of Asia (Fig. 2c). Shi et al. (2021) found that when NAO index is high, the temperature in the north of East Asia is high and that in the south is low. Li et al. (2022) found that southern East Asian temperatures are low when WP is low. This is consistent with our SATA results. The SATA in the phase of NAO-/WP- is strong (Fig. 2d), this phase results SATA decreases 2–4°C in north of Eastern Asia. NAO-/WP- phase forms an anomalous

Table 1. Classification of years by four phases

Phase	Year
NAO+/WP+	1983, 1988, 1989, 1993, 1994, 1999, 2001, 2002, 2006, 2007, 2008, 2013, 2016, 2017, 2018, 2019, 2020
NAO-/WP-	1985, 1996, 1997, 2010, 2011
NAO+/WP-	1980, 1981, 1982, 1984, 1986, 1990, 1991, 1992, 1995, 2000, 2004, 2005, 2012, 2014, 2015
NAO-/WP+	1987, 1998, 2003, 2009, 2021

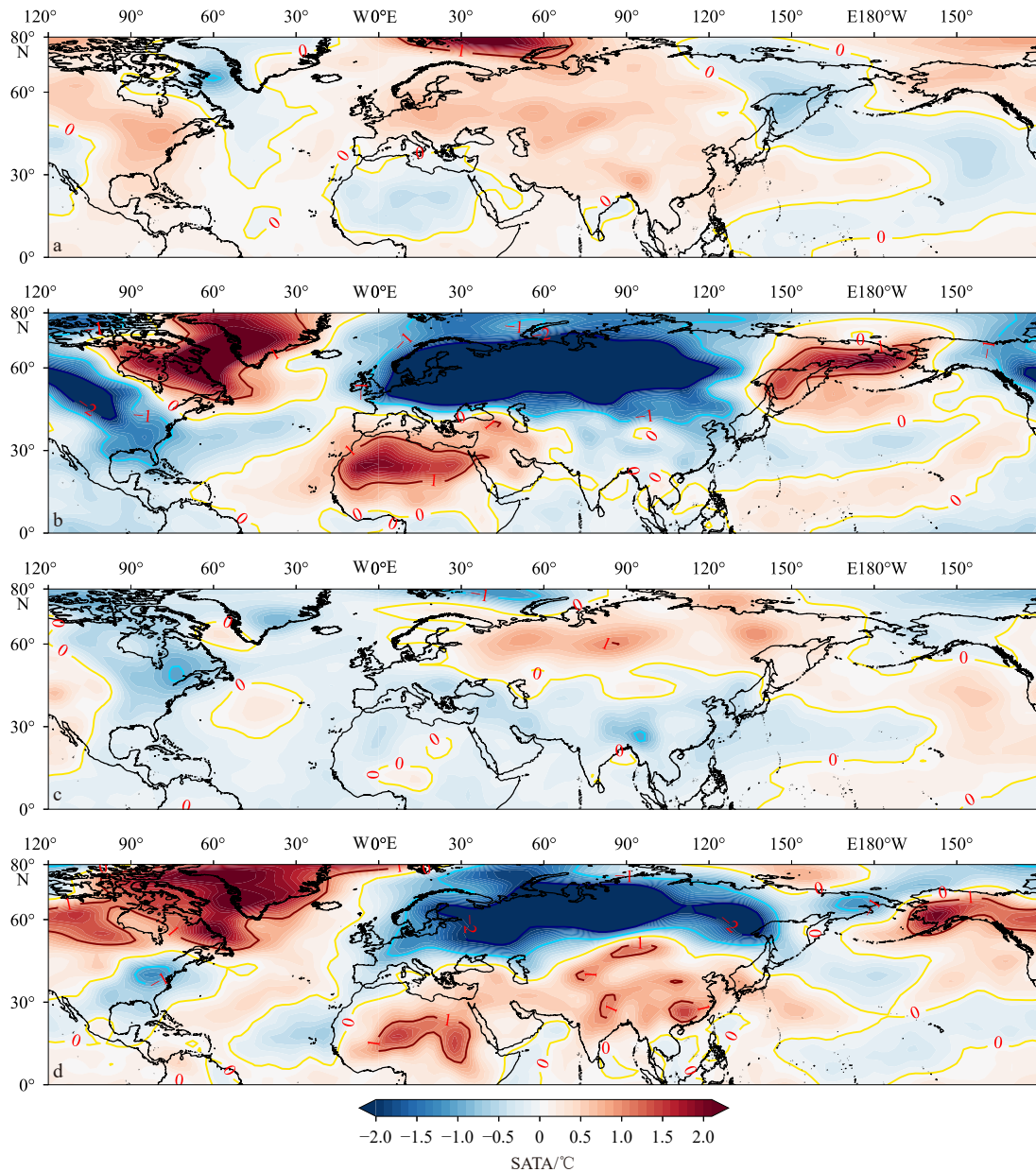


Fig. 2. The SATA in the four phases of 1980–2021 (DJF) (unit: °C). The SATA in the NAO+/WP+ phase (a); the SATA in the NAO-/WP- phase (b); the SATA in the NAO+/WP- phase (c); the SATA in the NAO-/WP+ phase (d).

warming center in the North Pacific, and cold area distributes in Northern Europe and Siberia. Meanwhile, SATA rises 0.8–1.3°C in southern Asia in the phase of NAO-/WP-. In terms of the distribution of SATA from Figs 2b and c, the temperatures are roughly opposite.

In Fig. 2, the winter temperature in Eastern Asia is roughly divided into two types under the four phases of NAO and WP. NAO+/WP- and NAO-/WP+ cause the different temperature between the north of Eastern Asian and south of it. The SATA is roughly opposite of NAO+/WP+ and NAO-/WP-.

3.2 The dynamic mechanism of SATA in the four phases

To explain the reason for the SATA distribution in the four phases of NAO-WP, we use the GH and wind field anomalies at 500 hPa to analyze the dynamic mechanism respectively (Fig. 3).

In phase of NAO+/WP+, the GH forms a north-south warping

plate pressure structure in the north of the Pacific (Fig. 3a). The pressure structure caused by NAO is the same as WP in the north of Atlantic (Fig. 3a). The structures cause the warm air continually entering the Eurasia trough from the mid-latitude Atlantic Ocean. Owing to high pressure in the south, the cold air is difficult to spread south. Thus, from the wind fields anomalies, the warm air gathers in Eurasia, and increases the temperature of the Eastern Asia (Fig. 2a). For the phase of NAO-/WP-, the effects of NAO-WP are relatively strong (Fig. 3b). Two high GH regions in northern Eurasia form cyclones respectively, then a pressure trough is formed over the Urals and Siberia, causing Arctic cold air spread to south. This cold air spreads over the low GH area of southern Eurasia, causing temperatures to decrease. According to the wind fields, a large of cold airflow from the Arctic into Siberia, causing low temperature in this region. At the same time, a cyclone is formed near the Kamchatka, it carries the cold air

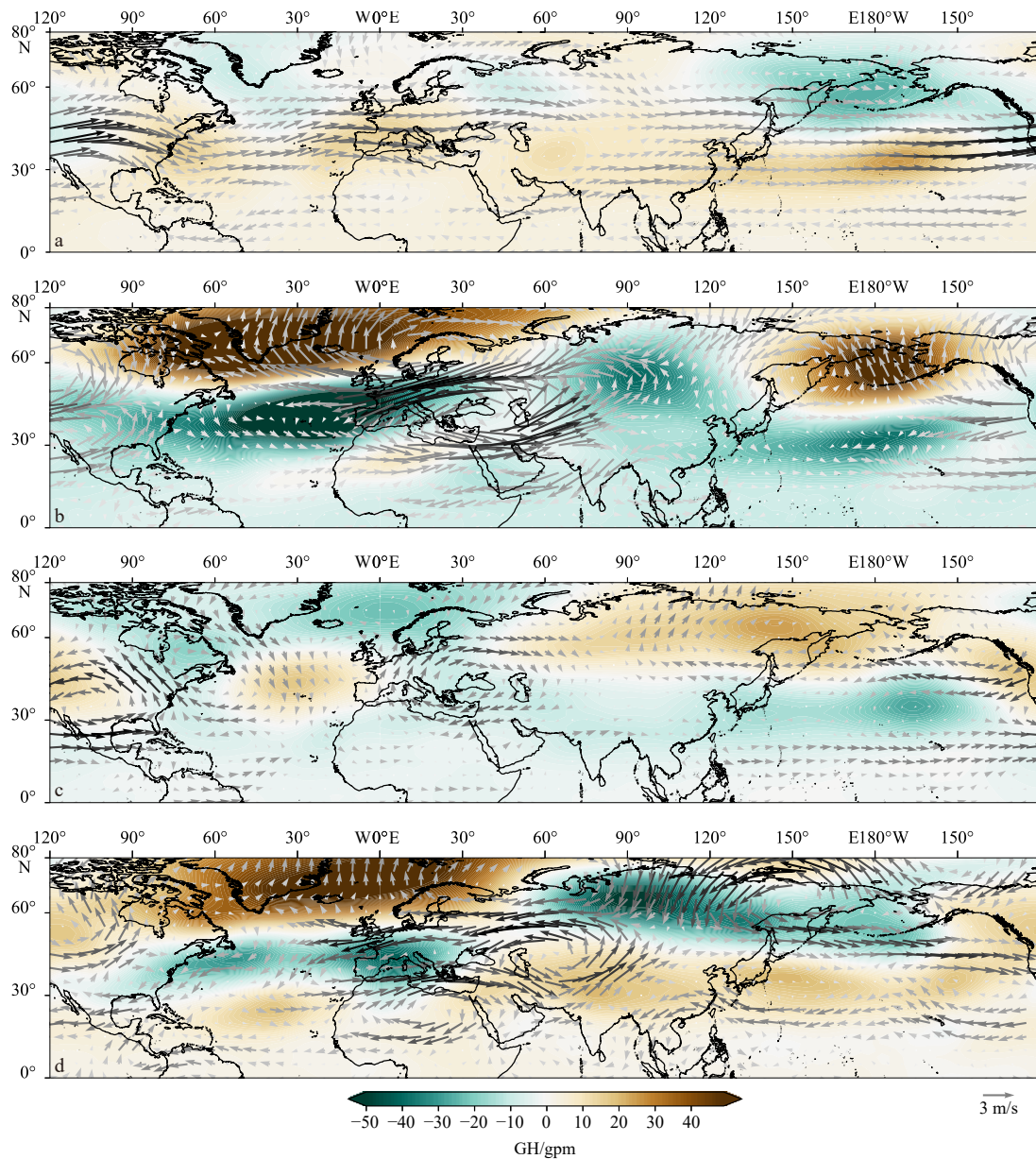


Fig. 3. The distribution of 500 hPa GH and wind field anomalies in the four phases of NAO-WP. The color respects the GH anomalies, arrows represent wind field. The NAO+/WP+ phase (a); the NAO-/WP- phase (b); the NAO+/WP- phase (c); the NAO-/WP+ phase (d).

southward and cools southeastern China.

For the phase of NAO+/WP-, there is a high GH anomaly over East Siberian Plateau, and high GH anomaly is formed by NAO over the Azores (Fig. 3c). High GH regions form cyclones to transport low-latitude warm air northward and block cold air. At the same time, although NAO weakens the jet stream, a cyclone transports cold air into the continent, and results in the temperature decrease in the south of Eurasia. The phase of NAO-/WP- is opposite to NAO+/WP- (Fig. 3d). In Eastern Asia, low GH forms cyclones in the north of Eastern Asia, and cold air from the Arctic spreads south. From the wind field anomalies, high pressure in the south transports warm air from low latitudes of the Pacific to the mainland, causing temperatures to rise. Two cyclones are formed by NAO on the western side of Eurasia, the airflow collides with cold air which is from Siberia, to block them from spreading south. After the collision of the airflow, a part of cold air spreads to Europe, and another transport to the east. As a result, the tem-

perature is decreased in northern Asia.

The Atlantic, Asian, and Pacific form an ocean-continent-ocean structure (Fig. 4). Under this structure, the NAO-WP phases affect the airflow by the pressure, and form different airflow-transport paths, then influence the winter temperatures finally.

In the phase of NAO+/WP+, high GH stays in the south of Eurasia (Fig. 4a). Warm westerly winds from the NAO in the Atlantic transport into Eurasia, with the high pressure structure of WP raises temperature in the south of Eastern Asia (Fig. 4a). However, in the phase of NAO-/WP-, high GH in the north of Asia blocks the warm air that from the low-latitude area (Fig. 4b). The cold air is transported to the south when the high GH area locates in the north of Eurasia. Strong wind anomalies cause cooling in the south of Eastern Asia. Differently, the east-west warped plate pressure structure formed by GH causes airflow collisions, when the phase of NAO is different from the phase of WP. Such as the

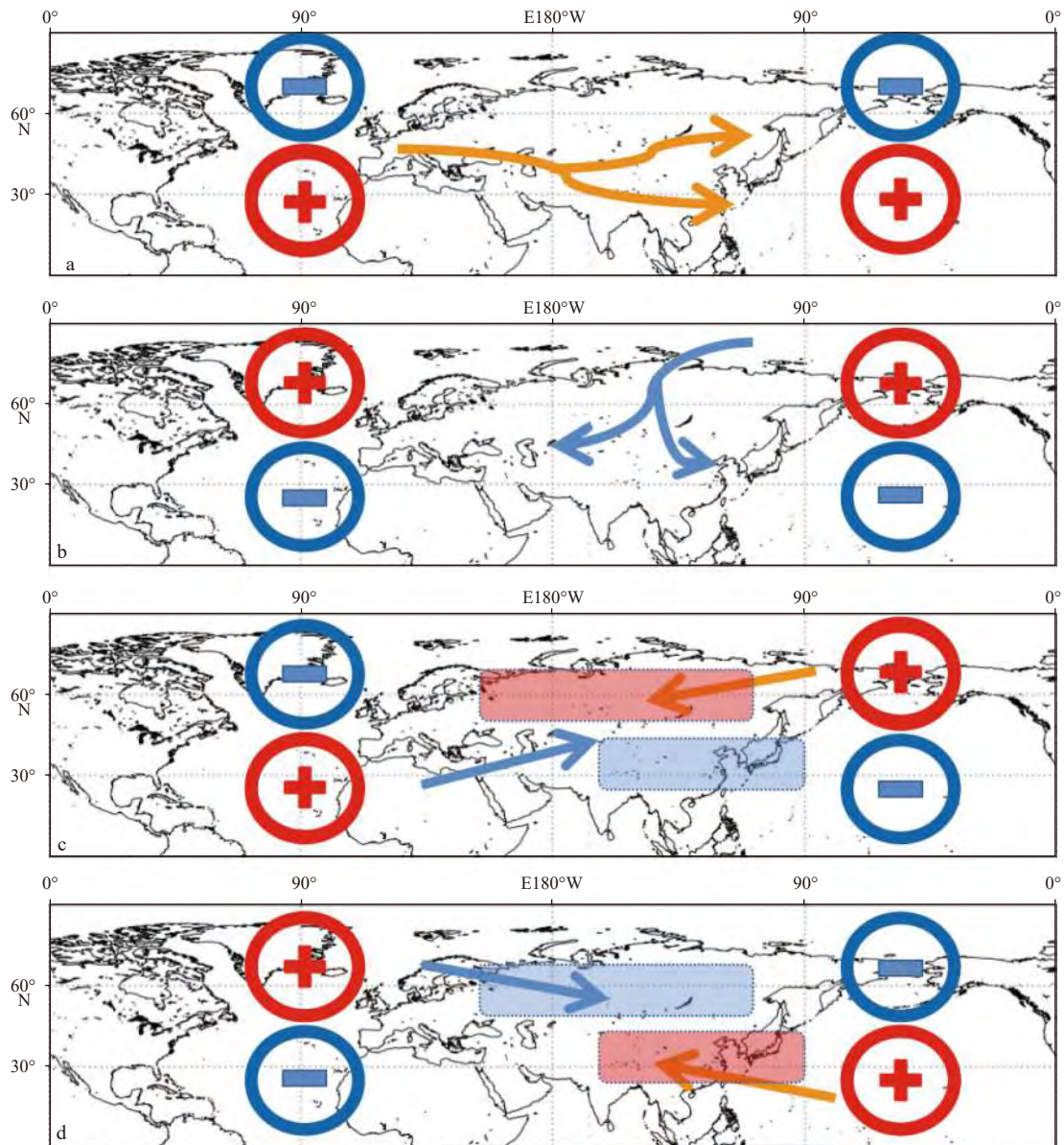


Fig. 4. A mechanism diagram showing the combined effects of NAO-WP phases. The NAO+/WP+ phase (a); the NAO-/WP- phase (b); the NAO+/WP- phase (c); the NAO-/WP+ phase (d).

phase of NAO+/WP-, the pressure adjusted by WP transports warm air from the Pacific, raising temperatures in northern Asia (Fig. 4c, red box). The pressure adjusted by NAO transports cold air from the Atlantic, and temperature is decreased in southern Asia (Fig. 4c, blue box). The airflow is transported by NAO and WP collides in central Eurasia. After collision, warm air transported by WP continues westward to impact Europe, and cold air transported by NAO continues eastward to Eastern Asia.

For the phase of NAO-/WP+, warm air is transported by WP from the Pacific, raises temperatures in south of Eastern Asia (Fig. 4d, red box). Cold air is transported by NAO from the Atlantic, then temperature is decreased in Europe (Fig. 4d, blue box). Unlike the phase of NAO+/WP-, the phase of NAO-/WP+ relies on high pressure to block the cold or warm air entry, therefore temperature is decreased or raised at different locations in Eurasia.

Under the action of NAO and WP, GH plays a dominant adjustable role. GH is the driving source of abnormal wind field.

Wind fields carry cold and warm air, causing temperatures to drop or rise. At the same time, GH also plays a role in blocking airflow, which is obvious in NAO-/WP-.

3.3 The regression and EOF of NAO-WP in the four phases

To measure the combined effect of the NAO-WP phase, multiple linear regression is established to discuss the relationship between the four phases of NAO-WP and the SATA. Considering the same phase, in the phase of NAO+/WP+, the NAO coefficients in north of Eastern Asia are mostly positive (Fig. 5a), and the WP coefficients are mostly negative value (Fig. 5b). Thus, the NAO and WP offset the impact on SATA. In the NAO-/WP- phases, the NAO coefficients in Eastern Asia (Fig. 5c) are opposite to the coefficient distribution of WP (Fig. 5d), the combined effect of NAO and WP are also weakened. The regression coefficients show that NAO and WP are weakened by each other in the phase of NAO+/WP+ and NAO-/WP-.

In the phases of NAO+/WP- and NAO-/WP+, the coefficients

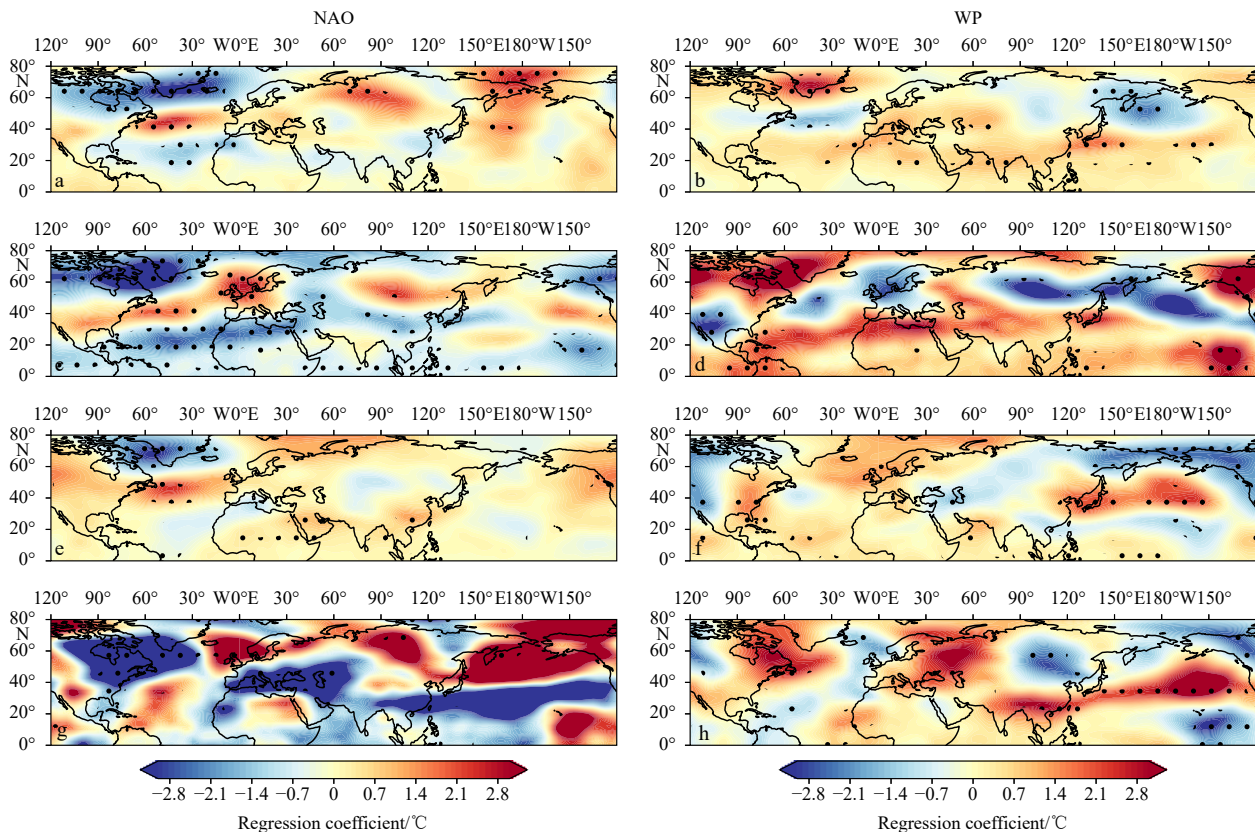


Fig. 5. The regression coefficients of NAO-WP with SATA in the four phases. a. The NAO regression coefficients of NAO+/WP+; b. the WP regression coefficients of NAO+/WP+; c. the NAO regression coefficients of NAO-/WP-; d. the WP regression coefficients of NAO-/WP-; e. the NAO regression coefficients of NAO+/WP-; f. the WP regression coefficients of NAO+/WP-; g. the NAO regression coefficients of NAO-/WP+; h. the WP regression coefficients of NAO-/WP+. The areas significant at the 95% confidence level are dotted.

of NAO regressed on SATA is not significant in Eastern Asia (Figs 5e and g), while it is significant for WP (Figs 5f and h). The reason shows that NAO has not a direct impact on the temperature in Eastern Asia. For other interference factors, further work needs to be discussed.

Furthermore, we analyze the annual variation of temperature in Eastern Asia by EOF method, in order to understand the annual variability of the NAO-WP in this region clearly. As shown in the Fig. 6, the EOF1 is similar to the phase of NAO-/WP+ in the Eastern Asia (Fig. 6a). The character of EOF1 mode is a meridional dipole with one low-temperature center over the Siberia and one high-temperature center over the south of Eastern Asia. Associated with the PC1 trends (Fig. 6b), this phase will continue appearing in the future. This abnormal cold center in Siberia could cause that the cold air spreads to southward. The EOF2 modes (Fig. 6c) are similar structures to the NAO-/WP-. In the northern part of Eurasia, there is a clear cold temperate zone, which shows cold air is raging in this high-latitude area. Relative to PC1, the trend of PC2 is not obvious (Fig. 6d). EOF3 accounts for only 8.16% (Fig. 6e), and PC3 shows fluctuating with annual variability (Fig. 6f). The influence of EOF3 mode is rare. In Eastern Asia, a clear high-temperature region can be seen. When the PC3 value is negative, the temperature are decreased in this region.

4 Conclusions

This study discusses the combined effects of four NAO-WP phases in NH. The phases of NAO-WP affect the airflow by air pressure, then it forms different air-transport paths for cold and

warm airflow and affects the winter temperature in the Eastern Asia finally.

In the phase of NAO+/WP+, a high pressure blocks the cold air from the Arctic and causes temperature increase in south of Eastern Asia. The impact of positive NAO is weak on Eastern Asia. WP sends the Pacific warm airflow into the Asian continent, then the SATA increases in south of East Asia. In the phase of NAO-/WP-, a high-pressure locates in north of Eastern Asia. Negative NAO forms a low-pressure zone in Europe, and forms a cold zone through Eurasia. Active cold airflow collides in Central Asia, causing the cold air to spread southward. Then the airflow causes the winter to become cold in Eastern Asia. In the phase of NAO+/WP-, Northern Asia is controlled by high pressure. Positive phase of NAO sends North Atlantic cold air into the Eurasia. The low pressure formed by WP causes temperature to decrease in Eastern Asia. In the phase of NAO-/WP+, the WP forms a low pressure in northern Asia, the cold air in the north causes the winter become colder, while the temperature increases in Southern Asia.

At present, the individual studies of NAO and WP about winter temperature are relatively plentiful. But the synergistic effects between NAO and WP are worth to be noticed. Different types of NAO-WP have different influence on temperature in Eastern Asia. As global warming, future climate predictions have become more volatile. The occurrence of extreme weather pose more threats and challenges to human survival. Studying the phases of NAO-WP and improving the predictive ability for SATA are valuable. Through the discussion on the relation of the SATA

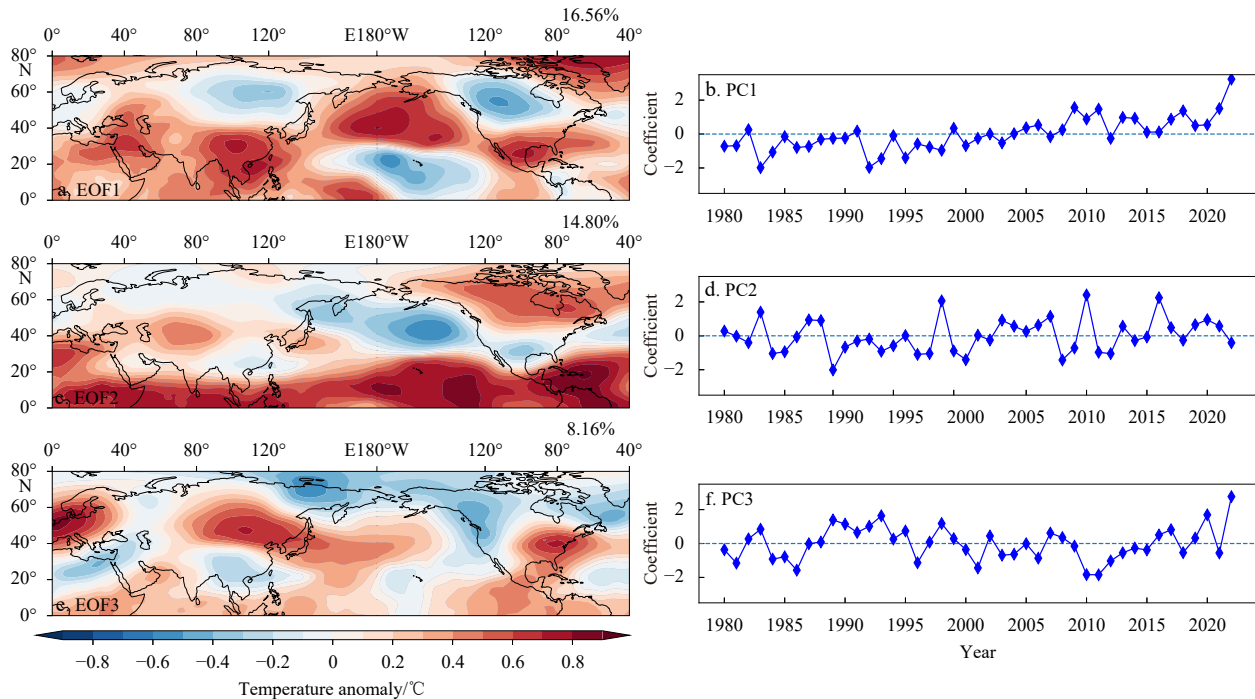


Fig. 6. The EOF modes of temperature anomalies (unit: $^{\circ}\text{C}$). The EOF analysis is performed by monthly 500 hPa air temperature in the region of NH, during DJF from 1979 to 2021. The percentages of variance explained by EOF modes are given in the upper right corner. The right panel is the corresponding PC time series for the EOF.

variability in winter with the GH and wind field anomaly, this study helps advance our understanding of the synergistic effect of NAO and WP on SATA for winter in Eastern Asia.

Acknowledgements

We thank our colleagues who contributed to drafting the manuscript. NCEP reanalysis derived data provided by the NOAA/OAR/ESRL PSL, Boulder, Colorado, USA, from the web site at https://www.psl.noaa.gov/data/gridded/data.20thC_ReanV3.html.

References

- Bell C J, Gray L J, Charlton-Perez A J, et al. 2009. Stratospheric communication of El Niño teleconnections to European winter. *Journal of Climate*, 22(15): 4083–4096, doi: [10.1175/2009jcli2717.1](https://doi.org/10.1175/2009jcli2717.1)
- Chen Wen, Lan Xiaoqing, Wang Lin, et al. 2013. The combined effects of the ENSO and the Arctic Oscillation on the winter climate anomalies in East Asia. *Chinese Science Bulletin*, 58(12): 1355–1362, doi: [10.1007/s11434-012-5654-5](https://doi.org/10.1007/s11434-012-5654-5)
- Dai Ying, Feldstein S B, Tan Benkui, et al. 2017. Formation mechanisms of the Pacific-North American teleconnection with and without its canonical tropical convection pattern. *Journal of Climate*, 30(9): 3139–3155, doi: [10.1175/JCLI-D-16-0411.1](https://doi.org/10.1175/JCLI-D-16-0411.1)
- Feldstein S B. 2000. The timescale, power spectra, and climate noise properties of teleconnection patterns. *Journal of Climate*, 13(24): 4430–4440, doi: [10.1175/1520-0442\(2000\)013<4430:TTPSAC>2.0.CO;2](https://doi.org/10.1175/1520-0442(2000)013<4430:TTPSAC>2.0.CO;2)
- Gong Daoyi, Wang Shaowu, Zhu Jinhong. 2001. East Asian winter monsoon and Arctic Oscillation. *Geophysical Research Letters*, 28(10): 2073–2076, doi: [10.1029/2000GL012311](https://doi.org/10.1029/2000GL012311)
- Hori M E. 2003. NAO impact towards the springtime snow disappearance in the western Eurasian continent. *Geophysical Research Letters*, 30(19): 1977, doi: [10.1029/2003GL018103](https://doi.org/10.1029/2003GL018103)
- Hurrell J W. 1995. Decadal trends in the North Atlantic Oscillation: Regional temperatures and precipitation. *Science*, 269(5224): 676–679, doi: [10.1126/science.269.5224.676](https://doi.org/10.1126/science.269.5224.676)
- Hurrell J W, Kushnir Y, Ottersen G, et al. 2003. An overview of the North Atlantic Oscillation. In: *The North Atlantic Oscillation: Climatic Significance and Environmental Impact*. Geophysical Monograph Series. American Geophysical Union, 134: 1–35, doi: [10.1029/134GM01](https://doi.org/10.1029/134GM01)
- Li Jianping, Wang Julian X L. 2003. A new North Atlantic Oscillation index and its variability. *Advances in Atmospheric Sciences*, 20(5): 661–676, doi: [10.1007/BF02915394](https://doi.org/10.1007/BF02915394)
- Li Jianping, Xie Tiejun, Tang Xinxin, et al. 2022. Influence of the NAO on wintertime surface air temperature over East Asia: Multi-decadal variability and decadal prediction. *Advances in Atmospheric Sciences*, 39(4): 625–642, doi: [10.1007/s00376-021-1075-1](https://doi.org/10.1007/s00376-021-1075-1)
- Nakamura T, Hara M, Oshika M, et al. 2015. Impact of the winter North Atlantic Oscillation (NAO) on the Western Pacific (WP) pattern in the following winter through Arctic sea ice and ENSO. Part II: multi-model evaluation of the NAO–ENSO linkage. *Climate Dynamics*, 45(11): 3547–3562, doi: [10.1007/s00382-015-2556-7](https://doi.org/10.1007/s00382-015-2556-7)
- Oshika M, Tachibana Y, Nakamura T. 2015. Impact of the winter North Atlantic Oscillation (NAO) on the Western Pacific (WP) pattern in the following winter through Arctic sea ice and ENSO: part I-observational evidence. *Climate Dynamics*, 45(5): 1355–1366, doi: [10.1007/s00382-014-2384-1](https://doi.org/10.1007/s00382-014-2384-1)
- Park H J, Ahn J B. 2016. Combined effect of the Arctic Oscillation and the Western Pacific pattern on East Asia winter temperature. *Climate Dynamics*, 46(9): 3205–3221, doi: [10.1007/s00382-015-2763-2](https://doi.org/10.1007/s00382-015-2763-2)
- Rousi E, Rust H W, Ulbrich U, et al. 2020. Implications of winter NAO flavors on present and future European climate. *Climate*, 8(1): 13, doi: [10.3390/cli8010013](https://doi.org/10.3390/cli8010013)
- Saunders M A, Qian Budong. 2002. Seasonal predictability of the winter NAO from north Atlantic sea surface temperatures. *Geophysical Research Letters*, 29(22): 2049, doi: [10.1029/2002GL014952](https://doi.org/10.1029/2002GL014952)
- Shi Chunhua, Sun Weijia, Guo Dong. 2021. Synergistic effects of WP and NAO on winter surface temperature in southeastern China. *Transactions of Atmospheric Sciences (in Chinese)*, 44(3): 394–404, doi: [10.13878/j.cnki.dqkxb.20191227002](https://doi.org/10.13878/j.cnki.dqkxb.20191227002)

- Shi Neng, Zhu Qianguan. 1993. Interannual variations in the telecorrelation intensity indices and their remote response to the El Niño events in the northern winter half year. *Journal of Nanjing Institute of Meteorology* (in Chinese), 16(3): 130-138, doi: [10.13878/j.cnki.dqkxxb.1993.02.003](https://doi.org/10.13878/j.cnki.dqkxxb.1993.02.003)
- Thompson D W J, Wallace J M. 1998. The Arctic Oscillation signature in the wintertime geopotential height and temperature fields. *Geophysical Research Letters*, 25(9): 1297-1300, doi: [10.1029/98GL00950](https://doi.org/10.1029/98GL00950)
- Wallace J M, Gutzler D S. 1981. Teleconnections in the geopotential height field during the Northern Hemisphere winter. *Monthly Weather Review*, 109(4): 784-812, doi: [10.1175/1520-0493\(1981\)109<0784:TITGHF>2.0.CO;2](https://doi.org/10.1175/1520-0493(1981)109<0784:TITGHF>2.0.CO;2)
- Wang Yongbo, Shi Neng. 2001. Relation of North Atlantic Oscillation anomaly to China climate during 1951-1995. *Journal of Nanjing Institute of Meteorology* (in Chinese), 24(3): 315-322, doi: [10.13878/j.cnki.dqkxxb.2001.03.003](https://doi.org/10.13878/j.cnki.dqkxxb.2001.03.003)
- Wibig J. 1999. Precipitation in Europe in relation to circulation patterns at the 500 hPa level. *International Journal of Climatology*, 19(3): 253-269, doi: [10.1002/\(SICI\)1097-0088\(19990315\)19:3<253::AID-JOC366>3.0.CO;2-0](https://doi.org/10.1002/(SICI)1097-0088(19990315)19:3<253::AID-JOC366>3.0.CO;2-0)
- Yao Yao, Luo Dehai. 2016. The North Atlantic Oscillation (NAO) and Europe blocking and their impacts on extreme snowstorms: A review. *Advances in Earth Science* (in Chinese), 31(6): 581-594
- Yoo C, Johnson N C, Chang C H, et al. 2018. Subseasonal prediction of wintertime East Asian temperature based on atmospheric teleconnections. *Journal of Climate*, 31(22): 9351-9366, doi: [10.1175/JCLI-D-17-0811.1](https://doi.org/10.1175/JCLI-D-17-0811.1)
- Zhang Ziyin, Gong Daoyi, Hu Miao, et al. 2009. Anomalous winter temperature and precipitation events in southern China. *Journal of Geographical Sciences*, 19(4): 471-488, doi: [10.1007/s11442-009-0471-8](https://doi.org/10.1007/s11442-009-0471-8)